Model Order Reduction for Nanoelectronics Coupled Problems with Many Inputs

N. Banagaaya*, L. Feng*, W. Schoenmaker †, P. Meuris†, A. Wieers‡, R. Gillon‡, P. Benner*
*Max Planck Institute for Dynamics of Complex Technical Systems, Magdeburg, Germany
Email: {banagaaya, feng, benner}@mpi-magdeburg.mpg.de
†Magwel NV, Martelarenplein 13, B-3000 Leuven, Belgium
Email: {wim.schoenmaker, peter.meuris}@magwel.com
‡ON Semiconductor Belgium, Oudenaarde, Belgium
Email:{ Aarnout.Wieers, Renaud.Gillon}@onsemi.com

***Abstract*—This paper is concerned with Model Order Reduction (MOR) for nanoelectronics coupled problems with many inputs. Our main applications are electro-thermal coupled problems described by nonlinear quadratic differential-algebraic systems (DAEs). We present algorithms that combine the advantages of the splitting techniques for DAEs and the existing MOR methods for systems with many inputs such as sparse implicit projection (SIP) for RC/RLC networks and MOR based on the superposition principle.**

I. Introduction

The models for nanoelectronics coupled problems, such as electro-thermal (ET) coupled problems, are very large in scale, and have a large number of inputs. In practice, there might be hundreds or thousands of inputs due to the coupling. Despite the ever increasing computational power, simulation of such large-scale systems with many terminals in acceptable time is very difficult. The reduced-order models (ROMs) are desired to speed up the simulation and in turn, shorten the design cycle. It is well known that as the number of inputs increases, the efficiency of the traditional Krylov subspace based model order reduction (MOR) decreases, since the size of the ROM is proportional to the number of inputs [1]. This has led to the development of new MOR methods specifically for system with very many inputs. So far, most of the developed methods are focused on RC/RLC networks arising from circuit simulations. The most commonly used MOR for interconnect circuits with large numbers of terminals are the elimination based methods, e.g., pole analysis via congruence transformations (PACT) [2], time constant equilibration reduction (TICER) [3], sparse implicit projection (SIP) [4]. The basic idea of these methods, is to obtain ROMs by eliminating the internal nodes, in a way similar to sparse Gaussian elimination [5]. The resulting ROMs aim to match the first two moments of the transfer functions of the original systems. Since the reduction is achieved by eliminating the internal nodes, the efficiency of the elimination based methods is not limited by the number of inputs. A drawback of the elimination based methods is that the elimination will introduce a large number of fill-ins, which result in ROMs with dense matrices. The efficiency gained by reducing the number of nodes is reduced significantly due to the large fill-in. This has led to the development of alternative MOR methods, such as SparseRC [6], which employ sparsity control strategy such as appropriate fill-in reducing orderings and/or graph-partitioning. Most recently an efficient aggregating based MOR (AMOR) method [1] for interconnect circuits with many terminals was proposed, based on the observation that adjacent nodes of the interconnect circuits with almost the same voltage can be aggregated together as a super node. For the case of large resistor networks, the method of effective reduction of resistor networks (reduceR) was proposed in [5]. However, the size of the ROM obtained using the above MOR methods depends on the row rank of the input matrix which limits their applicability. More general MOR methods for many inputs have been introduced in [7], [8], [9]. In [7], [8], the superposition property of linear systems is used, then standard MOR is performed separately with respect to each column of the input matrix. However, the superposition property is only applicable for MOR of linear systems. In [8], the extended singular value decomposition based MOR (ESVDMOR) algorithm was applied to power grid models with many inputs. This method, first reduces the dimension of the column space of the input matrix before applying a standard MOR method. However, it is not applicable to the problems with input matrices whose column space dimension is unreducible. All the above MOR methods for systems with very many inputs were developed specifically for R/RC/RLC circuits. As far as we know, MOR for nonlinear ET coupled problems has been rarely discussed in the literature.

In this paper, we propose a MOR method for ET coupled problems with many inputs that combines the ideas of existing methods. Our innovation is how to deal with the coupling between the electrical and the thermal part. The rest of the paper is organized as follows. In Section II, we discuss a general MOR approach for ET coupled models, and show the difficulty when the number of the terminals become large. In addition, we study the approach of treating nonzero initial conditions. In Section III, we discuss the application of the SIP method to ET coupled problems with many inputs and name this approach SIP-ET method. Section IV, proposes another MOR technique based on the superposition principle, which we call the BDSM-ET method. The results of the proposed methods are applied to two models from industry are presented in Section V. Finally, we conclude our paper.

II. MOR of ET coupled problems

Spatial discretization using the finite element method (FEM), finite volume method (FVM), or finite integration technique (FIT) of ET coupled problems leads to a nonlinear

978-3-9815370-6-2/DATE16/

quadratic dynamical system of the following form,

$$\mathbf{E}\boldsymbol{x}' = \mathbf{A}\boldsymbol{x} + \boldsymbol{x}^{\mathrm{T}}\mathbf{F}\boldsymbol{x} + \mathbf{B}\boldsymbol{u},\ \boldsymbol{x}(0) = \boldsymbol{x}_0, \tag{1a}$$

$$\boldsymbol{y} = \mathbf{C}\boldsymbol{x} + \mathbf{D}\boldsymbol{u}, \tag{1b}$$

where $\mathbf{E} \in \mathbb{R}^{n\times n}$ is singular, indicating that the system in (1) is a differential-algebraic equation (DAE). $\mathbf{A} \in \mathbb{R}^{n\times n}$, $\mathbf{B} \in \mathbb{R}^{n\times m}$, $\mathbf{C} \in \mathbb{R}^{\ell\times n}$, $\mathbf{D} \in \mathbb{R}^{\ell\times m}$, and the tensor $\mathbf{F} = \left[\mathbf{F}_1^{\mathrm{T}}, \ldots, \mathbf{F}_n^{\mathrm{T}}\right]^{\mathrm{T}}$ is a 3-D array of n matrices $\mathbf{F}_i \in \mathbb{R}^{n\times n}$. Each element in $\boldsymbol{x}^{\mathrm{T}}\mathbf{F}\boldsymbol{x} \in \mathbb{R}^n$ is a scalar $\boldsymbol{x}^{\mathrm{T}}\mathbf{F}_i\boldsymbol{x} \in \mathbb{R}, i = 1, \ldots, n$. The state vector $\boldsymbol{x} = (\boldsymbol{x}_v^{\mathrm{T}}, \boldsymbol{x}_T^{\mathrm{T}})^{\mathrm{T}} \in \mathbb{R}^n$ includes the nodal voltages $\boldsymbol{x}_v \in \mathbb{R}^{n_v}$, and the nodal temperatures $\boldsymbol{x}_T \in \mathbb{R}^{n_T}$. $\boldsymbol{u} = \boldsymbol{u}(t) \in \mathbb{R}^m$ and $\boldsymbol{y} = \boldsymbol{y}(t) \in \mathbb{R}^\ell$ are the inputs (excitations) and the desired outputs (observations), respectively. In order to ensure the uniqueness and existence of the solution of (1), the matrix pencil $\lambda\mathbf{E} - \mathbf{A}$ must be regular for every $\lambda \in \mathbb{C}$, that is, the polynomial $\mathcal{P}(\lambda) = \det(\lambda\mathbf{E} - \mathbf{A})$ is not identically zero. In this paper, we assume (1) has regular matrix pencil unless otherwise stated. In order to obtain accurate models, fine meshes must be used which lead to very large n compared to the number of inputs m and desired outputs ℓ. In [10], it was proposed that the best way to reduce coupled problems in the form of (1) is to first decouple them into algebraic (electrical) and differential (thermal) parts. Then, apply MOR to the differential and algebraic parts separately. Taking advantage of the natural structures of the matrices $\mathbf{E} = \begin{pmatrix} 0 & 0 \\ 0 & \mathbf{E}_v \end{pmatrix}$, $\mathbf{A} = \begin{pmatrix} \mathbf{A}_v & 0 \\ 0 & \mathbf{A}_T \end{pmatrix}$, $\mathbf{B} = \begin{pmatrix} \mathbf{B}_v \\ \mathbf{B}_T \end{pmatrix}$, $\mathbf{C} = \begin{pmatrix} \mathbf{C}_v & \mathbf{C}_T \end{pmatrix}$ and the tensor $\mathbf{F}$, we obtain the following decoupled algebraic (electrical) and differential (thermal) parts

$$0 = \mathbf{A}_v\boldsymbol{x}_v + \mathbf{B}_v\boldsymbol{u}, \tag{2a}$$

$$\mathbf{E}_T\boldsymbol{x}_T' = \mathbf{A}_T\boldsymbol{x}_T + \boldsymbol{x}_v^{\mathrm{T}}\mathbf{F}_T\boldsymbol{x}_v + \mathbf{B}_T\boldsymbol{u},\ \boldsymbol{x}_T(0) = \boldsymbol{x}_{T_0}, \tag{2b}$$

$$\boldsymbol{y} = \mathbf{C}_v\boldsymbol{x}_v + \mathbf{C}_T\boldsymbol{x}_T + \mathbf{D}\boldsymbol{u}, \tag{2c}$$

where $\mathbf{A}_v \in \mathbb{R}^{n_v\times n_v}$, $\mathbf{B}_v \in \mathbb{R}^{n_v\times m}$, $\mathbf{E}_T, \mathbf{A}_T \in \mathbb{R}^{n_T\times n_T}$, $\mathbf{B}_T \in \mathbb{R}^{n_T\times m}$ and $\mathbf{F}_T \in \mathbb{R}^{n_v\times n_v\times n_T}$. Equations (2a) and (2b) are the electrical and thermal parts, respectively. The dimension of (2a) can be reduced by eliminating internal nodes (to be discussed in Section III-A). The system in (2b) can be seen as a linear system, with the coupled term (the tensor) being treated as an extra input, through which the electrical states contribute to the thermal part. Therefore, it can be reduced using the standard Krylov subspace based MOR methods if the number of inputs m is small.

Since the initial condition of the differential part (2b) is nonzero, we need to first transform system (2b) with $\tilde{\boldsymbol{x}}_T = \boldsymbol{x}_T - \boldsymbol{x}_{T_0}$ [11], such that the standard Krylov subspace based MOR methods can be applied. Applying MOR to the transformed system results in a ROM of (2) as below,

$$0 = \mathbf{A}_{v_r}\boldsymbol{x}_{v_r} + \mathbf{B}_{v_r}\boldsymbol{u}, \tag{3a}$$

$$\mathbf{E}_{T_r}\boldsymbol{x}_{T_r}' = \mathbf{A}_{T_r}\boldsymbol{x}_T + \mathbf{V}_r^{\mathrm{T}}\boldsymbol{x}_{v_r}^{\mathrm{T}}\mathbf{F}_{T_r}\boldsymbol{x}_{v_r} + \mathbf{B}_{T_r}\tilde{\boldsymbol{u}}, \boldsymbol{x}_{T_r} = 0 \tag{3b}$$

$$\boldsymbol{y}_r = \mathbf{C}_{v_r}\boldsymbol{x}_{v_r} + \mathbf{C}_{T_r}\boldsymbol{x}_{T_r} + \mathbf{C}_T\boldsymbol{x}_{T_0} + \mathbf{D}\boldsymbol{u}, \tag{3c}$$

where $\mathbf{E}_{T_r} = \mathbf{V}_r^{\mathrm{T}}\mathbf{E}_T\mathbf{V}_r, \mathbf{A}_{T_r} = \mathbf{V}_r^{\mathrm{T}}\mathbf{A}_T\mathbf{V}_r \in \mathbb{R}^{r_2\times r_2}$, $\mathbf{B}_{T_r} = \mathbf{V}_r^{\mathrm{T}}\tilde{\mathbf{B}}_T \in \mathbb{R}^{r_2\times(m+1)}$, $\mathbf{B}_{v_r} \in \mathbb{R}^{r_1\times m}$, $\mathbf{A}_{v_r} \in \mathbb{R}^{r_1\times r_1}$, $\tilde{\mathbf{B}}_T = [\mathbf{B}_T, \mathbf{A}_T\boldsymbol{x}_{T_0}] \in \mathbb{R}^{n_T\times(m+1)}$, $\mathbf{F}_{T_r} \in \mathbb{R}^{r_1\times r_1\times n_T}$, $\tilde{\boldsymbol{u}} = [\boldsymbol{u}, 1]^{\mathrm{T}} \in \mathbb{R}^{m+1}$. The dimension of the ROM is $r = r_1 + r_2 \ll n$. Here, the projection matrix $\mathbf{V}_r$ can be constructed as an orthonormal basis of the Krylov subspace, i.e., $\mathrm{range}(\mathbf{V}_r) = \mathrm{span}\{\mathbf{R}, \mathbf{MR}, \cdots, \mathbf{M}^{r_2-1}\mathbf{R}\}$, $r_2 \ll n_T$, where $\mathbf{M} = (s_0\mathbf{E}_T - \mathbf{A}_T)^{-1}\mathbf{E}_T$, $\mathbf{R} = (s_0\mathbf{E}_T - \mathbf{A}_T)^{-1}\tilde{\mathbf{B}}_T$, and $s_0 \in \mathbb{C}$ is a properly chosen expansion point. A good reduced ET coupled model gives a small approximation error $\|\boldsymbol{y} - \boldsymbol{y}_r\|$ in a suitable norm $\|.\|$ for a large range of $\boldsymbol{u}$.

It can be seen from the above construction of $\mathbf{V}_r$ that, if the number of inputs m is very large, the many columns in the input matrix $\mathbf{B}$ lead to a projection matrix $\mathbf{V}_r$ with many columns, which will produce a ROM of large size. In the next section, we propose MOR methods which are potentially suitable for certain kinds of ET couple systems with many inputs.

III. Proposed SIP-ET method

In this section, we extend the idea of the SIP method for linear systems to ET coupled systems, and propose the SIP-ET method. The goal is to find a way of eliminating internal nodes while maintaining the electro-thermal coupling and the nonlinearity. It can be achieved by keeping the nodes connected to the external sources, and the nodes responsible for the coupling and the nonlinearity, and eliminating the rest.

A. Reduction of the algebraic part with many terminals using partitioning technique

We first partition (2a) by reordering the entries such that the first n_{v_e} rows correspond to the nonzero rows of the input matrix $\mathbf{B}_v$ and the rest n_{v_i} rows correspond to the internal nodes. Following this rule of partition, the system in (2a) can be rewritten into

$$\begin{aligned} 0 &= \begin{pmatrix} \mathbf{A}_{v_{11}} & \mathbf{A}_{v_{12}} \\ \mathbf{A}_{v_{12}}^{\mathrm{T}} & \mathbf{A}_{v_{22}} \end{pmatrix} \begin{pmatrix} \boldsymbol{x}_{v_e} \\ \boldsymbol{x}_{v_i} \end{pmatrix} + \begin{pmatrix} \mathbf{B}_{v_e} \\ 0 \end{pmatrix} \boldsymbol{u}, \\ \boldsymbol{y}_v &= \begin{pmatrix} \mathbf{C}_{v_e} & 0 \end{pmatrix} \begin{pmatrix} \boldsymbol{x}_{v_e} \\ \boldsymbol{x}_{v_i} \end{pmatrix}, \end{aligned} \tag{4}$$

where $\boldsymbol{x}_{v_e} \in \mathbb{R}^{n_{v_e}}$ and $\boldsymbol{x}_{v_i} \in \mathbb{R}^{n_{v_i}}$ represent the port nodal voltages and the internal nodal voltages, respectively, and $n_v = n_{v_e} + n_{v_i}$. $\mathbf{A}_{v_{11}} \in \mathbb{R}^{n_{v_e}\times n_{v_e}}$ and $\mathbf{A}_{v_{22}} \in \mathbb{R}^{n_{v_i}\times n_{v_i}}$ refer to the port and internal matrices, since they describe the branch interconnects between the port and internal nodes, respectively. $\mathbf{A}_{v_{12}} \in \mathbb{R}^{n_{v_e}\times n_{v_i}}$ is the connection matrix that describes the branches that connect internal nodes to port nodes. $\mathbf{B}_{v_e} \in \mathbb{R}^{n_{v_e}\times m}$ and $\mathbf{C}_{v_e} \in \mathbb{R}^{\ell\times n_{v_e}}$ are the nonzero blocks of matrices $\mathbf{B}_v$ and $\mathbf{C}_v$, respectively. In order to eliminate the internal nodes from (4), we use the fact that the internal nodes can be written in terms of the terminal nodes as

$$\boldsymbol{x}_{v_i} = -\mathbf{A}_{v_{22}}^{-1}\mathbf{A}_{v_{12}}^{\mathrm{T}}\boldsymbol{x}_{v_e}. \tag{5}$$

A ROM of (4) can be obtained by replacing $\boldsymbol{x}_{v_i}$ in (4) with the expression in terms of $\boldsymbol{x}_{v_e}$ in (5) as below,

$$\mathbf{A}_{v_r}\boldsymbol{x}_{v_r} = \mathbf{B}_{v_r}\boldsymbol{u}, \tag{6a}$$

$$\boldsymbol{y}_{v_r} = \mathbf{C}_{v_r}\boldsymbol{x}_{v_r}, \tag{6b}$$

where $\mathbf{A}_{v_r} = -\left[\mathbf{A}_{v_{11}} - \mathbf{A}_{v_{12}}\mathbf{A}_{v_{22}}^{-1}\mathbf{A}_{v_{12}}^{\mathrm{T}}\right]$, $\mathbf{B}_{v_r} = \mathbf{B}_{v_e}$, $\mathbf{C}_{v_r} = \mathbf{C}_{v_e}$, $\boldsymbol{x}_{v_r} = \boldsymbol{x}_{v_e}$, and $r_1 = n_{v_e} \ll n_v$. From (6a), we observe that the reduced matrix $-\mathbf{A}_{v_r}$ is the Schur compliment of the block $\mathbf{A}_{v_{22}}$ of the matrix $\mathbf{A}_v$. In practice,

the number n_{v_e} is usually much smaller than the number n_{v_i} of the internal unknowns, which leads to a huge reduction, in general. This is based on the assumption that the row rank of the input matrix $\mathbf{B}_v$ is very small compared to its dimension n_v. However the Schur complement is dense due to the large number of fill-ins. In many cases, eliminating all internal nodes is not advisable because it produces a ROM (6) with very dense matrix $\mathbf{A}_{v_r}$, which may even be more computationally expensive than the original model. Instead of eliminating all internal nodes, sparse control algorithms such as reduceR [5], have been proposed which minimizes fill-ins in the reduced matrix $\mathbf{A}_{v_r}$ by using fill-in reducing reordering algorithms, e.g., approximation minimum degree (AMD) [12], so that internal nodes responsible for fill-in are placed toward the end of the elimination sequence, along with the other nodes.

B. Reduction of differential part with many terminals using partitioning technique

Before applying MOR to the differential part in (2b), we need to replace the state $\boldsymbol{x}_v$ in the coupled term in (2b) with the reduced state $\boldsymbol{x}_{v_e}$, as the algebraic part is already reduced in Section III-A. Partitioning the state of the algebraic part as in (4), results in the decomposition of the nonlinear part $\boldsymbol{x}_v^{\mathrm{T}}\mathbf{F}_T\boldsymbol{x}_v$ in (2b) as below,

$$\boldsymbol{x}_v^{\mathrm{T}}\mathbf{F}_T\boldsymbol{x}_v = \boldsymbol{x}_{v_e}^{\mathrm{T}}\mathbf{F}_{T_{11}}\boldsymbol{x}_{v_e} + \boldsymbol{x}_{v_i}^{\mathrm{T}}\mathbf{F}_{T_{21}}\boldsymbol{x}_{v_e} + \boldsymbol{x}_{v_e}^{\mathrm{T}}\mathbf{F}_{T_{12}}\boldsymbol{x}_{v_i} + \boldsymbol{x}_{v_i}^{\mathrm{T}}\mathbf{F}_{T_{22}}\boldsymbol{x}_{v_i}, \quad (7)$$

where $\mathbf{F}_{T_{11}} \in \mathbb{R}^{n_{v_e}\times n_{v_e}\times n_T}$, $\mathbf{F}_{T_{12}} \in \mathbb{R}^{n_{v_e}\times n_{v_i}\times n_T}$, $\mathbf{F}_{T_{22}} \in \mathbb{R}^{n_{v_i}\times n_{v_i}\times n_T}$ and $\mathbf{F}_{T_{21}} \in \mathbb{R}^{n_{v_i}\times n_{v_e}\times n_T}$. Substituting (5) into (7) gives

$$\boldsymbol{x}_v^{\mathrm{T}}\mathbf{F}_T\boldsymbol{x}_v = \boldsymbol{x}_{v_e}^{\mathrm{T}}\mathbf{F}_{T_e}\boldsymbol{x}_{v_e}, \quad (8)$$

where $\mathbf{F}_{T_e} \in \mathbb{R}^{n_{v_e}\times n_{v_e}\times n_T}$ is a tensor defined as

$$\mathbf{F}_{T_e} = \mathbf{F}_{T_{11}} - \mathbf{W}_v^{\mathrm{T}}\mathbf{F}_{T_{21}} - \mathbf{F}_{T_{12}}\mathbf{W}_v + \mathbf{W}_v^{\mathrm{T}}\mathbf{F}_{T_{22}}\mathbf{W}_v,$$

with $\mathbf{W}_v = \mathbf{A}_{v_{22}}^{-1}\mathbf{A}_{v_{12}}^{\mathrm{T}} \in \mathbb{R}^{n_{v_i}\times n_{v_e}}$. Here, $\mathbf{W}^T\mathbf{F}_{T_{21}}$ means $\mathbf{W}_v^T$ multiplies each matrix block $\mathbf{F}_{T_{21}}^i \in \mathbb{R}^{n_{v_i}\times n_{v_e}}$ in $\mathbf{F}_{T_{21}}$ from the left, for $i = 1,\ldots,n_T$. Similarly, $\mathbf{F}_{T_{12}}\mathbf{W}_v$ means $\mathbf{W}_v$ multiplies each matrix block $\mathbf{F}_{T_{12}}^i \in \mathbb{R}^{n_{v_e}\times n_{v_i}}$ in $\mathbf{F}_{T_{12}}$ from the right, and $\mathbf{W}_v^T\mathbf{F}_{T_{22}}\mathbf{W}_v = \left[\mathbf{W}_v^T\mathbf{F}_{T_{22}}^{1^{\mathrm{T}}}\mathbf{W}_v,\ldots,\mathbf{W}_v^T\mathbf{F}_{T_{22}}^{{n_T}^{\mathrm{T}}}\mathbf{W}_v\right]^{\mathrm{T}}$, where $\mathbf{F}_{T_{22}}^i \in \mathbb{R}^{n_{v_i}\times n_{v_i}}$. Substituting (8) into (2b) leads to

$$\begin{aligned}\mathbf{E}_T\boldsymbol{x}_T' &= \mathbf{A}_T\boldsymbol{x}_T + \boldsymbol{x}_{v_e}^{\mathrm{T}}\mathbf{F}_{T_e}\boldsymbol{x}_{v_e} + \mathbf{B}_T\boldsymbol{u},\ \boldsymbol{x}_T(0) = \boldsymbol{x}_{T_0},\\ \boldsymbol{y}_T &= \mathbf{C}_T\boldsymbol{x}_T.\end{aligned} \quad (9)$$

We are now ready to apply MOR to the differential part in (9). For clarity, we rewrite the nonlinear part $\boldsymbol{x}_{v_e}^{\mathrm{T}}\mathbf{F}_{T_e}\boldsymbol{x}_{v_e}$ as $\boldsymbol{x}_{v_e}^{\mathrm{T}}\mathbf{F}_{T_e}\boldsymbol{x}_{v_e} = \mathbf{H}_{T_e}\boldsymbol{x}_{v_e}\otimes\boldsymbol{x}_{v_e}$, where $\mathbf{H}_{T_e} \in \mathbb{R}^{n_T\times n_{v_e}^2}$. Thus, (9) can be written as

$$\begin{aligned}\mathbf{E}_T\boldsymbol{x}_T' &= \mathbf{A}_T\boldsymbol{x}_T + \mathbf{H}_{T_e}\boldsymbol{x}_{v_e}\otimes\boldsymbol{x}_{v_e} + \mathbf{B}_T\boldsymbol{u},\\ \boldsymbol{y}_T &= \mathbf{C}_T\boldsymbol{x}_T,\end{aligned} \quad (10)$$

with initial condition $\boldsymbol{x}_T(0) = \boldsymbol{x}_{T_0}$. Using the state space transformation $\tilde{\boldsymbol{x}}_T = \boldsymbol{x}_T - \boldsymbol{x}_{T_0}$ gives the

$$\mathbf{E}_T\tilde{\boldsymbol{x}}_T' = \mathbf{A}_T\tilde{\boldsymbol{x}}_T + \mathbf{H}_{T_e}\boldsymbol{x}_{v_e}\otimes\boldsymbol{x}_{v_e} + \tilde{\mathbf{B}_T}\tilde{\boldsymbol{u}}, \quad (11a)$$

$$\boldsymbol{y}_T = \mathbf{C}_T\tilde{\boldsymbol{x}}_T + \mathbf{C}_T\boldsymbol{x}_{T_0}, \quad (11b)$$

with initial condition $\tilde{\boldsymbol{x}}_T(0) = 0$, where $\tilde{\boldsymbol{u}} = [\boldsymbol{u}, 1]^{\mathrm{T}} \in \mathbb{R}^{m+1}$ and $\tilde{\mathbf{B}}_T = [\mathbf{B}_T, \mathbf{A}_T\boldsymbol{x}_{T_0}] \in \mathbb{R}^{n_T\times(m+1)}$. Similar techniques of partitioning introduced in Section II-A can be applied to (11), such that the first n_{T_e} rows correspond to the maximum of the row ranks of the matrices $\mathbf{H}_{T_e}$ and $\tilde{\mathbf{B}}_T$, while the rest n_{T_i} rows correspond to the internal nodes. The partitioned system can be formulated as

$$\begin{pmatrix}\mathbf{E}_{T_{11}} & 0\\ 0 & \mathbf{E}_{T_{22}}\end{pmatrix}\begin{pmatrix}\boldsymbol{x}_{T_e}\\ \boldsymbol{x}_{T_i}\end{pmatrix}' = \begin{pmatrix}\mathbf{A}_{T_{11}} & \mathbf{A}_{T_{12}}\\ \mathbf{A}_{T_{12}}^{\mathrm{T}} & \mathbf{A}_{T_{22}}\end{pmatrix}\begin{pmatrix}\boldsymbol{x}_{T_e}\\ \boldsymbol{x}_{T_i}\end{pmatrix} + \begin{pmatrix}\mathbf{h}_{T_e}\\ 0\end{pmatrix}\boldsymbol{x}_{v_e}\otimes\boldsymbol{x}_{v_e} + \begin{pmatrix}\tilde{\mathbf{B}}_{T_e}\\ 0\end{pmatrix}\boldsymbol{u}, \quad (12a)$$

$$\boldsymbol{y}_T = \begin{pmatrix}\mathbf{C}_{T_e} & 0\end{pmatrix}\begin{pmatrix}\boldsymbol{x}_{T_e}\\ \boldsymbol{x}_{T_i}\end{pmatrix} + \begin{pmatrix}\mathbf{C}_{T_e} & 0\end{pmatrix}\begin{pmatrix}\boldsymbol{x}_{T_{0_e}}\\ \boldsymbol{x}_{T_{0_i}}\end{pmatrix}, \quad (12b)$$

where $\boldsymbol{x}_{T_e} \in \mathbb{R}^{n_{T_e}}$ and $\boldsymbol{x}_{T_i} \in \mathbb{R}^{n_{T_i}}$ represent the port nodal temperatures and the internal nodal temperatures, respectively, and $n_T = n_{T_e} + n_{T_i}$. $\mathbf{E}_{T_{11}} \in \mathbb{R}^{n_{T_e}\times n_{T_e}}$ and $\mathbf{A}_{T_{11}} \in \mathbb{R}^{n_{T_e}\times n_{T_e}}$ refer to the port matrices, since they describe the branch interconnects between the port nodal temperatures. $\mathbf{E}_{T_{22}} \in \mathbb{R}^{n_{T_i}\times n_{T_i}}$ and $\mathbf{A}_{v_{22}} \in \mathbb{R}^{n_{v_i}\times n_{v_i}}$ refer to the internal matrices, describing the branch interconnections between internal nodal temperatures. The matrix $\mathbf{A}_{T_{12}} \in \mathbb{R}^{n_{v_e}\times n_{v_i}}$ is the connection matrix that describes the branches connecting the internal nodes to the port nodes. $\mathbf{B}_{T_e} \in \mathbb{R}^{n_{T_e}\times m}$, $\mathbf{C}_{T_e} \in \mathbb{R}^{\ell\times n_{T_e}}$ and $\mathbf{h}_{T_e} \in \mathbb{R}^{n_{T_e}\times n_{v_e}^2}$ are the nonzero blocks of the matrices $\tilde{\mathbf{B}}_T$, $\mathbf{C}_T$ and $\mathbf{H}_{T_e}$, respectively. Following the idea in [6], we introduce a congruence transform $\mathbf{X}_c = \begin{pmatrix}\mathrm{I} & 0\\ -\mathbf{A}_{T_{22}}^{-1}\mathbf{A}_{T_{12}}^{\mathrm{T}} & \mathrm{I}\end{pmatrix}$ which isolates and eliminates the unwanted nodes so as to reduce the size of the thermal part in (12). More specifically, we apply the congruence transform $\mathbf{X}_c$ to (12), and obtain

$$\tilde{\mathbf{E}}_T\tilde{\tilde{\boldsymbol{x}}}_T' = \tilde{\mathbf{A}}_T\tilde{\tilde{\boldsymbol{x}}}_T + \tilde{\mathbf{H}}_{T_e}\boldsymbol{x}_{v_e}\otimes\boldsymbol{x}_{v_e} + \tilde{\tilde{\mathbf{B}}}_T\tilde{\boldsymbol{u}}, \quad (13a)$$

$$\boldsymbol{y}_T = \tilde{\mathbf{C}}_T\tilde{\tilde{\boldsymbol{x}}}_T + \mathbf{C}_T\boldsymbol{x}_{T_0}, \quad (13b)$$

where

$$\tilde{\mathbf{E}}_T = \mathbf{X}_c^{\mathrm{T}}\mathbf{E}_T\mathbf{X}_c = \begin{pmatrix}\mathbf{E}_{T_{11}} + \mathbf{W}_T^{\mathrm{T}}\mathbf{E}_{T_{22}}\mathbf{W}_T & -\mathbf{W}_T^{\mathrm{T}}\mathbf{E}_{T_{22}}\\ -\mathbf{E}_{T_{22}}\mathbf{W}_T & \mathbf{E}_{T_{22}}\end{pmatrix},$$

$$\tilde{\mathbf{A}}_T = \mathbf{X}_c^{\mathrm{T}}\mathbf{A}_T\mathbf{X}_c = \begin{pmatrix}\mathbf{A}_{T_{11}} - \mathbf{W}_T^{\mathrm{T}}\mathbf{A}_{T_{12}}^{\mathrm{T}} & 0\\ 0 & \mathbf{A}_{T_{22}}\end{pmatrix},$$

$$\tilde{\mathbf{H}}_{T_e} = \mathbf{X}_c^{\mathrm{T}}\mathbf{H}_{T_e} = \begin{pmatrix}\mathbf{h}_{T_e}\\ 0\end{pmatrix},\ \tilde{\tilde{\mathbf{B}}}_T = \mathbf{X}_c^{\mathrm{T}}\tilde{\mathbf{B}}_T = \begin{pmatrix}\tilde{\mathbf{B}}_{T_e}\\ 0\end{pmatrix},$$

$$\tilde{\mathbf{C}}_T = \mathbf{C}_T\mathbf{X}_c = \begin{pmatrix}\mathbf{C}_{T_e}\\ 0\end{pmatrix} \text{ and } \mathbf{W}_T = \mathbf{A}_{T_{22}}^{-1}\mathbf{A}_{T_{12}}^{\mathrm{T}}.$$ The main idea of the above transformation is to transform $\mathbf{A}_T$ into a block diagonal matrix $\tilde{\mathbf{A}}_T$ whose block size corresponds to the numbers n_{T_e} and n_{T_i}, respectively. Finally, the desired projection matrix that reduces (12) is obtained by removing the columns of $\mathbf{X}_c$ corresponding to $\boldsymbol{x}_{T_i}$ given by $\mathbf{V}_r = \begin{pmatrix}\mathrm{I}\\ -\mathbf{W}_T\end{pmatrix}$. Thus, substituting $\boldsymbol{x}_T = \mathbf{V}_r\boldsymbol{x}_{T_r}$ into (12), we obtain the ROM of (9),

$$\begin{aligned}\mathbf{E}_{T_r}\boldsymbol{x}_{T_r}' &= \mathbf{A}_{T_r}\boldsymbol{x}_{T_r} + \mathbf{h}_{T_e}\boldsymbol{x}_{v_e}\otimes\boldsymbol{x}_{v_e} + \mathbf{B}_{T_r}\tilde{\boldsymbol{u}},\\ \boldsymbol{y}_{T_r} &= \mathbf{C}_{T_r}\boldsymbol{x}_{T_r} + \mathbf{C}_T\boldsymbol{x}_{T_0},\end{aligned} \quad (14)$$

where $\mathbf{E}_{T_r} = \mathbf{V}_r^{\mathrm{T}}\mathbf{E}_T\mathbf{V}_r = \mathbf{E}_{T_{11}} + \mathbf{W}_T^{\mathrm{T}}\mathbf{E}_{T_{22}}\mathbf{W}_T$, $\mathbf{A}_{T_r} = \mathbf{V}_r^{\mathrm{T}}\mathbf{A}_T\mathbf{V}_r = \mathbf{A}_{T_{11}} - \mathbf{W}_T^{\mathrm{T}}\mathbf{A}_{T_{12}}^{\mathrm{T}}$, $\mathbf{B}_{T_r} = \mathbf{V}_r^{\mathrm{T}}\mathbf{B}_T = \tilde{\mathbf{B}}_{T_e}$ and $\mathbf{C}_{T_r} = \mathbf{C}_T\mathbf{V}_r = \mathbf{C}_{T_e}$. We note that $\mathbf{h}_{T_e}\boldsymbol{x}_{v_e} \otimes \boldsymbol{x}_{v_e}$ can be rewritten into the tensor formulation defined as $\mathbf{h}_{T_e}\boldsymbol{x}_{v_e} \otimes \boldsymbol{x}_{v_e} = \boldsymbol{x}_{v_e}^{\mathrm{T}}\mathbf{f}_{T_e}\boldsymbol{x}_{v_e}$, where $\mathbf{f}_{T_e} \in \mathbb{R}^{n_{v_e}\times n_{v_e}\times n_{T_e}}$. As discussed in the SIP algorithm [4], no orthogonalization of the columns in the matrix $\mathbf{V}_r$ is required, since it will destroy sparsity.

From the above analysis, we can see that the proposed reduction approach is an extension of the SIP in [4], which takes the coupling term into consideration. The reduced algebraic system in (6) and (14), together with the output equation $\boldsymbol{y}_r = \boldsymbol{y}_{v_r} + \boldsymbol{y}_{T_r} + \mathbf{D}\boldsymbol{u}$, gives the desired ROM of (1). We call the extended SIP method for ET coupled models SIP-ET method.

C. Fast implementation of the SIP-ET method

In this subsection, we discuss a more efficient way of implementing the SIP-ET algorithm. The SIP-ET algorithm in its current form is restricted to small and medium systems or systems with very few internal nodes. For large-scale problems, more sophisticated implementations have to be adapted. As we have already discussed in Section III-A, removing all internal nodes is infeasible and may lead to ROMs with very dense matrices in the algebraic part. The same problem arises in the reduction of the differential part discussed in Section III-B. This is due to the fact that removing all internal nodes at once, makes the construction of the matrices $\mathbf{W}_v = \mathbf{A}_{v_{22}}^{-1}\mathbf{A}_{v_{12}}^{\mathrm{T}}$ and $\mathbf{W}_T = \mathbf{A}_{T_{22}}^{-1}\mathbf{A}_{T_{12}}^{\mathrm{T}}$ responsible for the reduction, either costly or infeasible, for large-scale application, since the matrices $\mathbf{A}_{v_{22}}$ and $\mathbf{A}_{T_{22}}$ can be very large due to a large number of internal nodes. In addition, it also leads to dense matrices in the ROM (14). However, as mentioned in Section III-A, a sparse ROM can be obtained by using appropriate reordering algorithms such as AMD [12].

The SIP-ET method inherits all the properties of the standard SIP, see [4] for more details. However, the SIP-ET ROMs are not always small enough, especially in the differential part (thermal part) as illustrated in Tables II and III in Section V. In Section IV, we propose an alternative method which is not limited by the number of removal internal nodes.

IV. Proposed BDSM-ET Method

In this section, the standard BDSM [9] for linear time invariant systems (LTI) with many terminals is extended to a MOR method for ET coupled systems, which is named as BDSM-ET. Based on the superposition principle, the BDSM method involves first splitting the input matrix of the original MIMO (multi-input multi-output) system into SIMO (single-input multi-output) subsystems, such that the standard MOR methods, e.g., Krylov subspace based MOR, can be applied to each subsystem. It is known that the superposition principle is only available for LTI systems. However, the system (9) with the nonlinear coupled term, can be considered as a LTI system w.r.t the temperature nodes $\boldsymbol{x}_T$. The coupled term $\boldsymbol{x}_{v_e}^T\mathbf{F}_{T_e}\boldsymbol{x}_{v_e}$ is treated as a part of the input, since it only depends on the electrical nodes $\boldsymbol{x}_v$. Therefore, we can still apply the superposition principle to the differential part (9) even if it is nonlinear w.r.t the electrical part.

We intend to apply the principle in two stages, first we use it to split the system (9) into nonlinear and linear subsystems. Assuming that the input matrix $\mathbf{B}_T$ has full column rank m, it can be split into $\mathbf{B}_T = \mathbf{B}_{T_1} + \mathbf{B}_{T_l}$, with $\mathbf{B}_{T_l} = \sum_{i=2}^{m}\mathbf{B}_{T_i}$, where $\mathbf{B}_{T_i}$ are column rank-1 matrices defined column wise as

$$\mathbf{B}_{T_i}(:,j) = \begin{cases}\mathbf{b}_{T_i} \in \mathbb{R}^{n_T}, & \text{if } i \neq j,\\ 0, & \text{otherwise,}\end{cases}$$

$i = 1,\ldots,m$. $\mathbf{b}_{T_i}$ is the single nonzero column of $\mathbf{B}_{T_i}$. By the superposition principle and using the above input matrix splitting, the system (9) can be decomposed into a nonlinear subsystem

$$\mathbf{E}_T\boldsymbol{x}'_{T_n} = \mathbf{A}_T\boldsymbol{x}_{T_n} + \boldsymbol{x}_{v_e}^{\mathrm{T}}\mathbf{F}_{T_e}\boldsymbol{x}_{v_e} + \mathbf{B}_{T_1}\boldsymbol{u}, \tag{15a}$$

$$\boldsymbol{y}_{T_n} = \mathbf{C}_T\boldsymbol{x}_{T_n}, \tag{15b}$$

with initial condition $\boldsymbol{x}_{T_n}(0) = \boldsymbol{x}_{T_0}$ and a LTI system

$$\mathbf{E}_T\boldsymbol{x}'_{T_l} = \mathbf{A}_T\boldsymbol{x}_{T_l} + \mathbf{B}_{T_l}\boldsymbol{u},\ \boldsymbol{x}_{T_l}(0) = 0, \tag{16a}$$

$$\boldsymbol{y}_{T_l} = \mathbf{C}_T\boldsymbol{x}_{T_l}, \tag{16b}$$

with $\boldsymbol{y}_T = \boldsymbol{y}_{T_n} + \boldsymbol{y}_{T_l}$. Note that the nonlinear part only depends on the electrical state, and can be seen as an input into the thermal system in (15), so that the superposition principle still applies. In fact, the nonlinear subsystem (15) can be rewritten as a SIMO system, since $\mathbf{B}_{T_1}\boldsymbol{u} = \mathbf{b}_{T_1}\boldsymbol{u}_1$, where $\boldsymbol{u} = [\boldsymbol{u}_1,\ldots,\boldsymbol{u}_m]^{\mathrm{T}} \in \mathbb{R}^m$.

The LTI system in (16) can be split into $m-1$ subsystems given by

$$\mathbf{E}_T\boldsymbol{x}'_{T_{l_i}} = \mathbf{A}_T\boldsymbol{x}_{T_{l_i}} + \mathbf{B}_{T_{l_i}}\boldsymbol{u},\ \boldsymbol{x}_{T_{l_i}}(0) = 0, \tag{17a}$$

$$\boldsymbol{y}_{T_{l_i}} = \mathbf{C}_T\boldsymbol{x}_{T_{l_i}},\ i = 1,\ldots,m-1, \tag{17b}$$

where $\mathbf{B}_{T_{l_i}} = \mathbf{B}_{T_{i+1}}$ and $\boldsymbol{y}_{T_l} = \sum_{i=1}^{m-1}\boldsymbol{y}_{T_{l_i}}$. Let blkdiag denotes the block-diagonal matrix from the input arguments, the LTI system in (16) can be reformulated as the parallel connection of the subsystems in (17) [9]. Consequently, it can be equivalently transformed into a block-diagonal system $(\mathcal{E}_{T_l}, \mathcal{A}_{T_l}, \mathcal{B}_{T_l}, \mathcal{C}_{T_l})$ of dimension $(m-1)n_T$ with matrix coefficients

$$\mathcal{E}_{T_l} = \mathrm{blkdiag}(\mathbf{E}_T,\ldots,\mathbf{E}_T),\ \mathcal{A}_{T_l} = \mathrm{blkdiag}(\mathbf{A}_T,\ldots,\mathbf{A}_T),$$
$$\mathcal{B}_{T_l} = (\mathbf{B}_{T_2}^{\mathrm{T}}\ldots\mathbf{B}_{T_m}^{\mathrm{T}})^{\mathrm{T}} \text{ and } \mathcal{C}_{T_l} = (\mathbf{C}_T\ldots\mathbf{C}_T). \tag{18}$$

Combining the nonlinear part in (15) with the LTI part in the block-diagonal form (18) leads to a block-diagonal system of dimension mn_T given by

$$\begin{pmatrix}\mathbf{E}_T & 0\\ 0 & \mathcal{E}_{T_l}\end{pmatrix}\tilde{\boldsymbol{x}}'_T = \begin{pmatrix}\mathbf{A}_T & 0\\ 0 & \mathcal{A}_{T_l}\end{pmatrix}\tilde{\boldsymbol{x}}_T + \boldsymbol{x}_{v_e}^{\mathrm{T}}\begin{pmatrix}\mathbf{F}_{T_e}\\ 0\end{pmatrix}\boldsymbol{x}_{v_e} + \begin{pmatrix}\mathbf{B}_{T_1}\\ \mathcal{B}_{T_l}\end{pmatrix}\boldsymbol{u},\ \tilde{\boldsymbol{x}}_T(0) = \begin{pmatrix}\boldsymbol{x}_{T_0}\\ 0\end{pmatrix}, \tag{19a}$$

$$\boldsymbol{y}_T = \begin{pmatrix}\mathbf{C}_T & \mathcal{C}_{T_l}\end{pmatrix}, \tag{19b}$$

where $\tilde{\boldsymbol{x}}_T = \begin{pmatrix}\boldsymbol{x}_{T_n}^{\mathrm{T}} & \tilde{\boldsymbol{x}}_l^{\mathrm{T}}\end{pmatrix}^{\mathrm{T}}$. This system is an equivalent model of the original differential part in (9).

In the following discussions, we assume $\boldsymbol{x}_{T_0} = 0$ for simplicity. Extension of the proposed MOR method to ET coupled

problems with nonzero initial conditions is straight forward. We try to apply MOR to the block diagonal system in (19) instead of (9). Since system (19) still has many inputs m, the standard Krylov subspace projection method, such as PRIMA [13], cannot be applied directly. Instead, we approximate $\tilde{\boldsymbol{x}}_T$ by $\tilde{\boldsymbol{x}}_T = \mathbf{V}\boldsymbol{x}_{T_r}$, with $\mathbf{V} = \text{blkdiag}(\mathbf{V}_n, \mathbf{V}_l) \in \mathbb{R}^{mn_T \times \tilde{r}}$ leading to the block-diagonal nonlinear ROM of (19) given by

$$\begin{pmatrix} \mathbf{E}_{T_r} & 0 \\ 0 & \mathcal{E}_{T_{l_r}} \end{pmatrix} \boldsymbol{x}'_{T_r} = \begin{pmatrix} \mathbf{A}_{T_r} & 0 \\ 0 & \mathcal{A}_{T_{l_r}} \end{pmatrix} \boldsymbol{x}_{T_r} + \mathbf{V}^{\mathrm{T}} \boldsymbol{x}_{v_e}^{\mathrm{T}} \begin{pmatrix} \mathbf{F}_{T_e} \\ 0 \end{pmatrix} \boldsymbol{x}_{v_e} + \begin{pmatrix} \mathbf{B}_{T_{1_r}} \\ \mathcal{B}_{T_{l_r}} \end{pmatrix} \boldsymbol{u},\ \boldsymbol{x}_{T_r}(0) = \begin{pmatrix} 0 \\ 0 \end{pmatrix}, \quad (20a)$$

$$\boldsymbol{y}_{T_r} = \begin{pmatrix} \mathbf{C}_{T_r} & \mathcal{C}_{T_{l_r}} \end{pmatrix}, \quad (20b)$$

where $\mathbf{E}_{T_r} = \mathbf{V}_n^{\mathrm{T}} \mathbf{E}_T \mathbf{V}_n, \mathbf{A}_{T_r} = \mathbf{V}_n^{\mathrm{T}} \mathbf{A}_T \mathbf{V}_n, \mathbf{C}_{T_r} = \mathbf{C}_T \mathbf{V}_n$, $\mathcal{B}_{T_{l_r}} = \mathbf{V}_l^{\mathrm{T}} \mathcal{B}_{T_l}, \mathbf{B}_{T_{1_r}} = \mathbf{V}_n^{\mathrm{T}} \mathbf{B}_{T_1}, \mathcal{E}_{T_{l_r}} = \mathbf{V}_l^{\mathrm{T}} \mathcal{E}_{T_l} \mathbf{V}_l$, $\mathcal{C}_{T_{l_r}} = \mathcal{C}_{T_l} \mathbf{V}_l$ and $\mathcal{A}_{T_{l_r}} = \mathbf{V}_l^{\mathrm{T}} \mathcal{A}_{T_l} \mathbf{V}_l$.

The projection matrices $\mathbf{V}_n$ and $\mathbf{V}_l$ can be constructed from the matrices $\mathbf{V}^{(i)}$ defined as below,

$$\text{range}(\mathbf{V}^{(i)}) = \text{span}\{\mathbf{r}_i, \mathbf{M}\mathbf{r}_i, \cdots, \mathbf{M}^{r-1}\mathbf{r}_i\},\ r \ll n_T,$$

where $\mathbf{M} = (s_0\mathbf{E}_T - \mathbf{A}_T)^{-1}\mathbf{E}_T$ and $\mathbf{r}_i = (s_0\mathbf{E}_T - \mathbf{A}_T)^{-1}\mathbf{b}_{T_i}$, $i = 1, \ldots m$. Finally, $\mathbf{V}_n = \mathbf{V}^{(1)}$ and $\mathbf{V}_l = \text{blkdiag}(\mathbf{V}^{(2)}, \mathbf{V}^{(3)}, \ldots, \mathbf{V}^{(m-1)})$. Here $\mathbf{b}_{T_i}$ is the single nonzero column in $\mathbf{B}_{T_i}$ and $s_0 \in \mathbb{C}$ is chosen arbitrary. The final ROM (20) of the differential part in (9) is of dimension $\tilde{r} = mr$. Combining the ROM (6) of the electrical part, the ROM (20) of the thermal part with the output equation $\boldsymbol{y}_r = \boldsymbol{y}_{v_r} + \boldsymbol{y}_{T_r} + \mathbf{D}\boldsymbol{u}$, we obtain the ROM of (1) based on the superposition principle. It is worth pointing out that, the proposed BDSM-ET method inherits the moment-matching property of the standard BDSM [9].

V. Numerical Experiments

In this section, we illustrate the robustness of our proposed SIP-ET and BDSM-ET methods by examining two ET coupled models from industrial applications, one is a package model with $n = 9193$ coupled equations, and the other is a device model with $n = 13216$ coupled equations. As discussed in this paper, we first decouple the system into electrical and thermal parts. In Table I, n_v and n_T are the numbers of nodal voltages and nodal temperatures, respectively. The dimension of the system is given by $n = n_v + n_T$. m and ℓ are the number of inputs and outputs respectively. Next, we compare the ROMs

TABLE I: Electro-thermal coupled models

Model (n)	n_v	n_T	ℓ	m
9193	8071	1122	68	34
13216	11556	1660	12	6

obtained using the SIP-ET and BDSM-ET methods for these models, as illustrated in Tables II and III. For the electrical part, we use the SIP method discussed in Section III-A, while for the thermal parts, we apply SIP-ET and BDSM-ET method, respectively. In Table II, we show the results for the cases with nonzero initial conditions while in Table III, we consider the cases with zero initial conditions.

We can observe that both methods leads to large ROMs, especially for the thermal part, if the original system has a nonzero initial condition. For the SIP-ET method, a nonzero column matrix is introduced in the input matrix caused by the nonzero initial condition, and as a result, the number of the zero rows in the input matrix is reduced, so that much fewer internal nodes can be eliminated, leading to a ROM of large size. Compared to the SIP-ET method, smaller ROMs are obtained by the BDSM-ET method, as illustrated in Tables II and III, since its reduction procedure is independent of the zero rows of the input matrix. However, the size of ROMs generated by the BDSM-ET method dependent on the number of inputs.

TABLE II: Non-zero initial condition $\boldsymbol{x}_0 \neq 0$, $r = r_1 + r_2$

	BDSM-ET ROM				SIP-ET ROM			
Model (n)	r_1	r_2	r	% Red	r_1	r_2	r	% Red
9193	188	2698	2886	68.6	188	6865	7053	23.3
13216	160	124	284	98.0	160	5422	5582	57.8

TABLE III: Zero initial condition $\boldsymbol{x}_0 = 0$, $r = r_1 + r_2$

	BDSM-ET ROM				SIP-ET ROM			
Model (n)	r_1	r_2	r	% Red	r_1	r_2	r	% Red
9193	188	187	375	96.0	188	1932	2120	76.9
13216	160	39	199	98.5	160	2700	2860	78.4

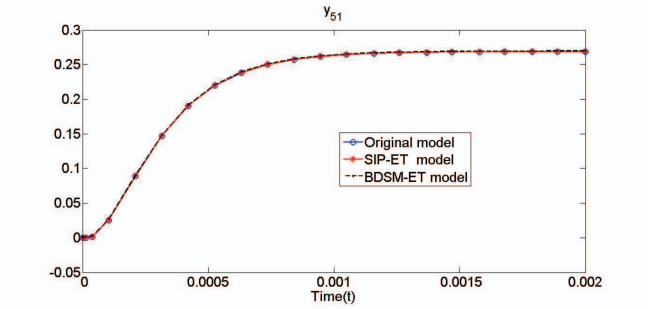

Fig. 1: Output solution $\boldsymbol{y}_{51}$, $\boldsymbol{x}_0 \neq 0$, $n = 9193$

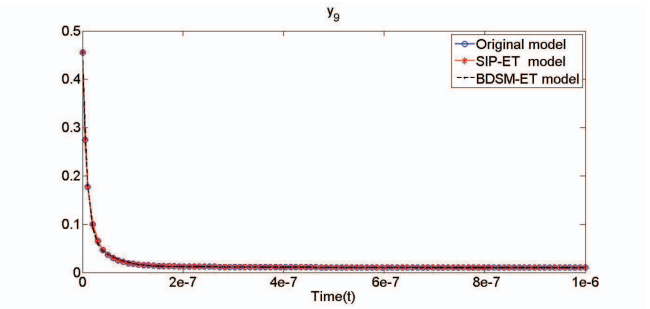

Fig. 2: Output solution $\boldsymbol{y}_9$, $\boldsymbol{x}_0 \neq 0$, $n = 13216$

All output solutions of the SIP-ET and BDSM-ET ROMs coincide with that of their respective original models. In

Figures 1 and 2, we compare one of the the output solutions of the SIP-ET and BDSM-ET ROMs with those of the original models. It can be seen that the solutions of all ROMs coincide with the original model up to an error below 10^{-3}.

VI. Conclusion

We have discussed MOR for ET coupled problems with many inputs. Two MOR methods, SIP-ET and BDSM-ET, for ET coupled problems with many inputs have been proposed. The algebraic (electrical) part is reduced using SIP, while the differential (thermal) part is reduced by employing the SIP approach and the BDSM approach, respectively. The advantage of the SIP-ET method is that its reduction procedure is independent of the number of input. However, it does not always lead to small ROMs. The BDSM-ET method depends on the number of inputs, but it has a block-diagonal structure that makes it computationally efficient.

Acknowledgment

This work is supported by the collaborative project nanoCOPS, Nanoelectronics COupled Problems Solutions, supported by the European Union in the FP7-ICT-2013-11 Program under Grant Agreement Number 619166.

References

[1] Y. Su, F. Yang, and X. Zeng, "AMOR: An efficient aggregating based model order reduction method for many-terminal interconnect circuits," in *Proc. Design Automation Conference*, 2012.

[2] K. Kerns and A. Yang, "Stable and efficient reduction of large, multiport RC networks by pole analysis via congruence transformations," *IEEE Trans. Comput.-Aided Design Integr. Circuits Syst.*, vol. 16, no. 7, pp. 734 – 744, 1997.

[3] B. Sheehan, "TICER: Realizable reduction of extracted RC circuits," in *Proc. International Conference on Computer-Aided Design*, 1999.

[4] Z. Ye, D. Vasilyev, Z. Zhu, and J. Phillips, "Sparse Implicit Projection (SIP) for reduction of general many-terminal networks," in *Proc. International Conference on Computer-Aided Design*, 2008.

[5] J. Rommes and W. Schilders, "Efficient Methods for Large Resistor Networks," *IEEE Trans. Comput.-Aided Design Integr. Circuits Syst.*, vol. 29, no. 1, pp. 28 – 39, 2010.

[6] R. Ionutiu, J. Rommes, and W. Schilders, "SparseRC: Sparsity Preserving Model Reduction for RC Circuits with Many Terminals," *IEEE Trans. Comput.-Aided Design Integr. Circuits Syst.*, vol. 30, no. 12, pp. 1828 – 1841, 2011.

[7] P. Benner, L. Feng, and E. Rudnyi, "Using the superposition property for model reduction of linear systems with a large number of inputs," in *the 18th International Symposium on Mathematical Theory of Networks & Systems*, 2008.

[8] P. Benner and A. Schneider, "Model Reduction for Linear Descriptor Systems with Many Ports," in *Progress in Industrial Mathematics at ECMI 2010*, ser. Mathematics in Industry, M. Günther, A. Bartel, M. Brunk, S. Schöps, and M. Striebel, Eds., vol. 17. Berlin: Springer-Verlag, 2012, pp. 137–143.

[9] Z. Zhang, C. C. X. Hu, and N. Wong, "A Block-Diagonal Structured Model Reduction Scheme for Power Grid Networks," in *Design, Automation & Test in Europe Conference & Exhibition (DATE)*, 2011.

[10] N. Banagaaya, L. Feng, P. Meuris, W. Schoenmaker, and P. Benner, "Model Order Reduction of an Electro-Thermal Package Model," in *proc. 8th Vienna International Conference on Mathematical Modelling (MathMod Vienna)*, F. Breitenecker, A. Kugi, and I. Troch, Eds., vol. 8, 2015, pp. 934–935.

[11] U. Baur, P. Benner, and L. Feng, "Model Order Reduction for Linear and Nonlinear Systems: A System-Theoretic Perspective," *Arch. Comput. Methods Eng.*, vol. 21, no. 4, pp. 331–358, 2014.

[12] P. Amestoy, T. Davis, and I. Duff, "An Approximate Minimum Degree Ordering Algorithm," *SIAM. J. Matrix Anal. & Appl.*, vol. 17, no. 4, pp. 886–905, 1996.

[13] A. Odabasioglu, M. Celik, and L. Pileggi, "PRIMA: passive reduced-order interconnect macromodeling algorithm," *IEEE Trans. Comput.-Aided Design Integr. Circuits Syst.*, vol. 17, no. 8, pp. 645–654, 1997.